# Anisotropic Hydrogel Thickness Gradient Films Derivatized to Yield Three-Dimensional Composite Materials

Xuejun Wang, Richard T. Haasch, and Paul W. Bohn*

*Department of Chemistry and Frederick Seitz Materials Research Laboratory, University of Illinois at Urbana-Champaign, 600 S. Mathews Avenue, Urbana, Illinois 61801*

*Received February 16, 2005*

We report the preparation of in-plane density gradients of amino-terminated molecules and gold particles through derivatization of laterally varying thickness gradients of poly(acrylic acid) (PAA) or poly(acrylamide) (PAAm) films. PAA and PAAm gradients were formed by Zn(II)-catalyzed electropolymerization of acrylic acid (AA) or acrylamide (AAm) in the presence of an in-plane electrochemical potential gradient applied to Au or indium−tin−oxide (ITO) working electrodes. PAA thickness gradients were converted into density gradients of fluorocarbons or biocompatible groups by derivatizing with $NH_2CH_2(CF_2)_6CF_3$ or an Arg-Gly-Asp (RGD)-containing peptide, respectively. X-ray photoelectron spectroscopy (XPS) and XPS imaging were used to characterize the modified PAA gradients. Transition regions as narrow as 104 $\mu$m were achieved for fluorocarbon gradients. PAAm gradients were treated with gold particles to form a density gradient of gold particles. Surface plasmon resonance imaging and scanning electron microscopy (SEM) as well as UV−visible absorption measurements were used to characterize the gold particle density gradients. It is likely that the gold particles were attached both on the surface and inside the PAAm film.

## Introduction

Recently, there has been a great deal of interest in generating and utilizing gradient surfaces because of their myriad possible applications, such as forming substrates for selective adsorption, templates for cell migration, and tools for combinatorial studies. A number of techniques for generating gradients on various substrates have been reported, including diffusion-controlled vapor deposition,[1] cross diffusion,[2,3] corona discharge,[4,5] photoimmobilization,[6,7] the use of microfluidic devices,[8,9] and, more recently, atom transfer radical polymerization (ATRP).[10−12] Surface-bound gradients of protein−nanoparticle conjugates on functionalized surfaces have also been generated by varying the contact time between solution-phase protein−metal nanoparticle conjugates and functionalized surfaces such as poly-L-lysine-coated glass slides.[13] Irrespective of the method of formation, the utility of anisotropic in-plane gradient surfaces scales directly with the range of chemical and physical properties that can be accessed and manipulated on gradient surfaces.

In our laboratory, an electrochemical-potential-gradient-based method has been developed to generate chemical composition gradients on thin Au electrodes.[14−21] In this method, in-plane current is injected at one end of an ultrathin (5 nm ≤ $d$ ≤ 80 nm) Au film and collected at the other end, while the Au film is used simultaneously as the working electrode of an electrochemical cell. The injection of currents yields significant in-plane potential drops so that, rather than assuming a single value of potential, an in-plane potential gradient, $V(x)$, is imposed on the working electrode surface according to

$$V(x) = V_0 + \int \frac{i\rho(l)}{A}\,\mathrm{d}l \qquad (1)$$

where $V_0$ is the potentiostat voltage offset, $i$ is the magnitude of the injected current, $\rho(l)$ is the film resistivity, and $A$ is the cross-sectional area of the Au working electrode. The in-plane potential gradient can be exploited to map organothiols onto the Au electrode surface by using characteristic reductive desorption/oxidative adsorption reactions of alkanethiols. In contrast to other preparation methods, this approach is not limited in physical size, it

* Corresponding author. E-mail: bohn@scs.uiuc.edu.

(1) Chaudhury, M. K.; Whitesides, G. M. *Science* **1992**, *256*, 1539−1541.
(2) Liedberg, B.; Tengvall, P. *Langmuir* **1995**, *11*, 3821−3827.
(3) Liedberg, B.; Wirde, M.; Tao, Y.-T.; Tengvall, P.; Gelius, U. *Langmuir* **1997**, *13*, 5329−5334.
(4) Jeong, B. J.; Lee, J. H.; Lee, H. B. *J. Colloid Interface Sci.* **1996**, *178*, 757−763.
(5) Lee, J. H.; Kim, H. G.; Khang, G. S.; Lee, H. B.; Jhon, M. S. *J. Colloid Interface Sci.* **1992**, *151*, 563−570.
(6) Hypolite, C. L.; McLernon, T. L.; Adams, D. N.; Chapman, K. E.; Herbert, C. B.; Huang, C. C.; Distefano, M. D.; Hu, W.-S. *Bioconj. Chem.* **1997**, *8*, 658−663.
(7) Herbert, C. B.; McLernon, T. L.; Hypolite, C. L.; Adams, D. N.; Pikus, L.; Huang, C. C.; Fields, G. B.; Letourneau, P. C.; Distefano, M. D.; Hu, W.-S. *Chem. Biol.* **1997**, *4*, 731−737.
(8) Jeon, N. L.; Dertinger, S. K. W.; Chiu, D. T.; Choi, I. S.; Stroock, A. D.; Whitesides, G. M. *Langmuir* **2000**, *16*, 8311−8316.
(9) Dertinger, S. K. W.; Jiang, X.; Li, Z.; Murthy, V. N.; Whitesides, G. M. *Proc. Natl. Acad. Sci. U.S.A.* **2002**, *99*, 12542−12547.
(10) Wu, T.; Efimenko, K.; Vlcek, P.; Subr, V.; Genzer, J. *Macromolecules* **2003**, *36*, 2448−2453.
(11) Bhat, R. R.; Tomlinson, M. R.; Genzer, J. *Macromol. Rapid Commun.* **2004**, *25*, 270−274.
(12) Bhat, R. R.; Genzer, J.; Chaney, B. N.; Sugg, H. W.; Liebmann-Vinson, A. *Nanotechnology* **2003**, *14*, 1145−1152.
(13) Kramer, S.; Xie, H.; Gaff, J.; Williamson, J. R.; Tkachenko, A. G.; Nouri, N.; Feldheim, D. A.; Feldheim, D. L. *J. Am. Chem. Soc.* **2004**, *126*, 5388−5395.
(14) Terrill, R. H.; Balss, K. M.; Zhang, Y.; Bohn, P. W. *J. Am. Chem. Soc.* **2000**, *122*, 988−989.
(15) Balss, K. M.; Coleman, B. D.; Lansford, C. H.; Haasch, R. T.; Bohn, P. W. *J. Phys. Chem. B* **2001**, *105*, 8970−8978.
(16) Balss, K. M.; Fried, G. A.; Bohn, P. W. *J. Electrochem. Soc.* **2002**, *149*, C450−C455.
(17) Balss, K. M.; Kuo, T.-C.; Bohn, P. W. *J. Phys. Chem. B* **2003**, *107*, 994−1000.
(18) Plummer, S. T.; Wang, Q.; Bohn, P. W.; Stockton, R.; Schwartz, M. A. *Langmuir* **2003**, *19*, 7528−7536.
(19) Plummer, S. T.; Bohn, P. W. *Langmuir* **2002**, *18*, 4142−4149.
(20) Wang, Q.; Bohn, P. W. *J. Phys. Chem. B* **2003**, *107*, 12578−12584.
(21) Wang, Q.; Jakubowski, J. A.; Sweedler, J. V.; Bohn, P. W. *Anal. Chem.* **2003**, *76*, 1−8.

10.1021/la0580053 CCC: $30.25 
Published on Web 07/28/2005

is easier to tune gradient properties such as transition position and slope, and the gradients may be altered after initial formation, thereby yielding spatial and temporal control over the surface composition, $\Gamma(x, y; t)$. The formation of electrochemical gradients is also not limited to the Au/alkanethiol system. For example, Hillier and Jayaraman formed Pt coverage gradients on an electronically conductive indium−tin−oxide (ITO) substrate by using the in-plane electrochemical potential gradient approach.[22]

Recently, we reported that this electrochemical approach can be extended to form a poly(acrylic acid) (PAA) thickness gradient on Au electrode surfaces by using the local potential, $V(x)$, to control the rate of electropolymerization.[23] Polymer hydrogels such as PAA and PAAm are of interest because of the wide range of stimuli that can be used to control their properties and their biocompatibility. For example, polymer hydrogels can change their volume and shape reversibly in response to external stimuli such as temperature, solvent composition, pH, ionic concentration, voltage, and light.[24−35] Crooks and co-workers demonstrated the versatility of hyperbranched PAA films by derivatizing them with molecules containing a wide range of moieties, such as fluorescent groups, ion-binding macrocycles, biocompatible polymer chains, and electroactive groups.[36] In the present work, we report that the as-formed PAA thickness gradient can be easily converted into density gradients of molecules containing a fluorocarbon group or a biological ligand (Arg-Gly-Asp peptide) through the formation of amide linkages. These two groups demonstrate the versatility of the PAA thickness gradient that results in surfaces in which physical properties ($\Gamma_{C-F} \approx$ surface tension) or biological recognition (RGD is the ligand for the integrin family of cell-surface receptors) is varied laterally. XPS imaging is used to characterize the gradient transition region of the fluorocarbon group density gradient because of the high sensitivity of the F 1s and Au 4f photoelectrons.

Furthermore, poly(acrylamide) (PAAm) thickness gradients can also be created on a Au electrode and ITO surfaces using the electrochemical approach. These PAAm thickness gradients are used as matrixes to create density gradients of Au nanoparticles. Genzer and co-workers reported that gold nanoparticles can be assembled into PAAm polymer brushes through electrostatic interactions.[12] They formed PAAm polymer brush gradients by varying the contact time between a solution-phase monomer and a surface-bound initiator. Here we explore the formation of chemically and mechanically stabilized PAAm films through chemical cross linking and the preparation of submillimeter-scale Au−nanoparticle derivatized PAAm gradient structures.

## Experimental Section

**Materials.** 11-Mercaptoundecanoic acid (MUA), acrylic acid, acrylamide, *N*-*N*′-methylenebisacrylamide, zinc chloride, pentafluorophenol (PFP), *N*-hydroxysuccinimide (NHS), and 1-ethyl-3-(dimethylamino)propylcarbodiimide (EDC) were purchased from Aldrich. 1H,1H-perfluorooctylamine (PFOA) was purchased from Lancaster Synthesis, Inc. Gly-Arg-Gly-Asp-Ser-Pro-Lys (GRGDSPK) peptide (RGD peptide, FW = 715.7 Da) was purchased from American Peptide Company, and methoxy poly(ethylene glycol)thiol, MW 2000, (PEG-SH) was purchased from Shearwater Corporation. Au colloids of 20-nm diameter were purchased from British Biocell International. Au colloids of 16-nm diameter were prepared by following a literature method.[37] KOH and HCl were purchased from Fischer Scientific. Absolute ethanol (EtOH) was purchased from Aaper Alcohol and Chemical Company. All reagents were used as received.

**Instrumentation.** UV−visible extinction spectra were acquired on a Cary 300 spectrophotometer. Scanning electron microscopy (SEM) imaging was performed on a Hitachi S-4700 scanning electron microscope under ultrahigh vacuum conditions, $\sim 10^{-9}$ Torr, using a field emission electron source. All images were collected at a 10-kV operating voltage.

**Substrate Preparation.** Microscope slides, cut into 13 mm × 8 mm pieces, and 60° SF-10 prisms (Spindler & Hoyer) were cleaned in piranha solution (concentrated $H_2SO_4$ and 30% $H_2O_2$ 3:1 in volume − *CAUTION: piranha solutions are strongly oxidizing and should not be allowed to contact organic solvents*) for 30 min and then were rinsed completely with copious amount of deionized (18.2 MΩ cm) water. The samples were then transferred to the evaporation chamber immediately to minimize contamination. The pressure in the vacuum chamber was maintained below $5 \times 10^{-8}$ Torr during the evaporation. An Au film, 50-nm-thick, was evaporated on the slides as a 10 mm × 3 mm, 6 mm × 1 mm, or 6 mm × 0.5 mm strip. For the 6 mm × 1 mm strip, two 150-nm-thick Au pads (3 mm × 3 mm) separated by 3 mm were evaporated over the strip to generate a 3 mm × 1 mm active region for gradient formation. For the 6 mm × 0.5 mm strip, two 150-nm-thick Au pads (3 mm × 3 mm) separated by 1 mm were evaporated over the strip to generate a 1 mm × 0.5 mm active region for gradient formation. An adhesion layer of Cr (1 nm) was deposited at the Au−glass interface for each layer. The deposition rates for Cr and Au were 0.03 and 1.5 Å/s, respectively. Samples were stored under $N_2$ before use. Prior to polymer formation, the samples were cleaned in piranha solution for 1 min, rinsed thoroughly with deionized water, rinsed again with EtOH, and dried with blown $N_2$. For surface plasmon resonance (SPR) imaging experiments, two 150-nm-thick Au pads separated by 25 mm were first evaporated on the prisms in order to maintain good contact. Then 45 nm of Au and a 1-nm Cr layer were deposited over the Au pads. The active gradient formation area was defined by the O-ring sealing the cell, which had a 12.5-mm diameter. Prior to polymer formation, the films were exposed to $O_3$ for 25 min, rinsed thoroughly with EtOH, and dried with $N_2$. $O_3$ was produced by passing $O_2$ at a low flow rate by a low-pressure Hg lamp upstream of the sample chamber.

**Formation of PAA and PAAm Thickness Gradients.** A bipotentiostat, employing a saturated Ag/AgCl reference electrode and a stainless steel counter electrode, was used to prepare the PAA and PAAm gradients. For PAA film growth, a 2.0 M acrylic acid aqueous solution with 0.04 M *N*,*N*′-methylenebisacrylamide and 0.2 M $ZnCl_2$ was used. For PAAm film growth, a 2.5 M acrylamide aqueous solution with 0.04 M *N*,*N*′-methylenebisacrylamide and 0.2 M $ZnCl_2$ was used. Contacts were made on two Au pads of the sample, one serving as working electrode E1 and the other as working electrode E2, by physically pressing Au wires against the respective electrode contact pads. Dynamic

(22) Jayaraman, S.; Hillier, A. C. *Langmuir* **2001**, *17*, 7857−7864.
(23) Wang, X. J.; Bohn, P. W. *J. Am. Chem. Soc.* **2004**, *126*, 6825−6832.
(24) Berndt, I.; Richtering, W. *Macromolecules* **2003**, *36*, 8780−8785.
(25) Kishi, R.; Miura, T.; Kihara, H.; Asano, T.; Shibata, M.; Yosomiya, R. *J. Appl. Polym. Sci.* **2003**, *89*, 75−84.
(26) Park, J. S.; Lee, H. J.; Choi, S. J.; Geckeler, K. E.; Cho, J.; Moon, S. H. *J. Colloid Interface Sci.* **2003**, *259*, 293−300.
(27) Yamashita, K.; Hashimoto, O.; Nishimura, T.; Nango, M. *React. Funct. Polym.* **2002**, *51*, 61−68.
(28) Katime, I.; Rodriguez, E. *J. Macromol. Sci., Pure Appl. Chem.* **2001**, *38*, 543−558.
(29) Dautzenberg, H.; Gao, Y. B.; Hahn, M. *Langmuir* **2000**, *16*, 9070−9081.
(30) Chiu, H. C.; Yang, C. H. *Polym. J.* **2000**, *32*, 574−582.
(31) White, B. H. B.; Kwak, J. C. T. *Colloid Polym. Sci.* **1999**, *277*, 785−791.
(32) Otake, K.; Karaki, R.; Ebina, T.; Yokoyama, C.; Takahashi, S. *Macromolecules* **1993**, *26*, 2194−2197.
(33) Kawasaki, H.; Sasaki, S.; Maeda, H. *J. Phys. Chem. B* **1997**, *101*, 5089−5093.
(34) Qiu, Y.; Park, K. *Adv. Drug Delivery Rev.* **2001**, *53*, 321−339.
(35) Kim, S. J.; Lee, K. J.; Kim, S. I.; Lee, Y. M.; Chung, T. D.; Lee, S. H. *J. Appl. Polym. Sci.* **2003**, *89*, 2301−2305.
(36) Bruening, M. L.; Zhou, Y. F.; Aguilar, G.; Agee, R.; Bergbreiter, D. E.; Crooks, R. M. *Langmuir* **1997**, *13*, 770−778.
(37) Makarova, O. V.; Ostafin, A. E.; Miyoshi, H.; Norris, J. R.; Meisel, D. *J. Phys. Chem. B* **1999**, *103*, 9080−9084.

PAA or PAAm thickness gradients were formed by performing potential cycling on one working electrode while maintaining a constant potential offset on the other electrode throughout the voltage program. Typically, for gold-covered glass samples, E1 was cycled five times between −1500 and +100 mV versus Ag/AgCl while keeping E2 at a potential 300 mV positive with respect to E1 throughout the experiment. For surface plasmon resonance (SPR) imaging experiments, contacts were made on two thick Au pads of the Au/prism surface by pressing Au wires to E1 and E2. A static PAAm gradient was formed by applying −1300 and −1100 mV constantly at the two ends of the active gradient region while acquiring SPR images. After gradient formation, the samples were treated with 0.1 M HCl for 10 min to dissolve metallic $Zn^0$ that accumulates in the hydrogel during deposition. The film was then rinsed with deionized water (18.2 MΩ cm, Milli Q UV-Plus system, Millipore), dried under a stream of nitrogen, and used immediately thereafter.

**Derivatization of PAA with PFOA.** The PAA thickness gradient film, prepared immediately before derivatization, was activated by soaking in NHS/EDC solution (75 mM EDC/15 mM NHS in 10 mM phosphate buffer, pH 6.0) for 1 h. After rinsing with 10 mM pH 6.0 phosphate buffer and then deionized water, the film was exposed to a solution of 0.1 M $NH_2CH_2(CF_2)_6CF_3$ in DMF.[36] After 1 h, the film was immediately rinsed in DMF and then rinsed in EtOH, dried under a stream of nitrogen, and used immediately or stored under dry nitrogen.

**Derivatization of PAA with RGD Peptide.** The RGD peptide was immobilized onto PAA films by modifying a published procedure.[38] Acrylic acid (2.0 M) in 50% EtOH/50% water with 0.04 M ethylene glycol dimethacrylate and 0.2 M $ZnCl_2$ was used for PAA film growth. Ethylene glycol dimethacrylate was used as the cross linker here, instead of *N*,*N*′-methylenebisacrylamide, to eliminate the interference in the N 1s photoelectron signal from the cross linker. Uniform PAA polymer films were formed by sweeping at 50 mV/s between −1500 and +100 mV versus Ag/AgCl 20 times. PAA thickness gradient films were formed by sweeping the potential of one end of the electrode at 50 mV/s between −1500 and +100 mV versus Ag/AgCl 20 times while maintaining a constant +300 mV offset at the other end of the working electrode. After gradient formation, the samples were treated with 0.1 M HCl for 10 min to dissolve metallic $Zn^0$ that accumulates in the hydrogel during deposition. The samples were then rinsed with deionized water, dried under a stream of nitrogen, and used immediately. Prior to RGD peptide modification, the PAA film was treated with 1 mM PEG-SH in deionized water for 1 h to avoid physical adsorption of peptide. The PAA film was rinsed with PBS and then with deionized water before being dried with a stream of nitrogen. The freshly prepared PAA films were then activated by immersing them in an ethanol solution of EDC (0.1 M) and PFP (0.2 M) for 30 min. After being rinsed with ethanol, the film was immersed in a solution of RGD peptide (1 mg/mL in PBS) for 1 h. The RGD peptide-derivatized film was first rinsed with PBS and then with deionized water before being dried with a stream of nitrogen and was used immediately or stored under dry nitrogen.

**Derivatization of PAAm with Au Nanoparticles.** Freshly prepared PAAm thickness gradient samples were treated with 0.1 M HCl for 10 min to dissolve metallic $Zn^0$ that accumulates in the hydrogel during deposition. The film was rinsed with deionized water, dried under a stream of nitrogen, and soaked in a Au colloid solution overnight. The sample was then rinsed with deionized water and dried with a stream of nitrogen.

**X-ray Photoelectron Spectroscopy (XPS).** X-ray photoelectron spectra were obtained using a Kratos Axis Ultra spectrometer with monochromatic Al Kα radiation at 1486.6 eV (225 W, 40 eV pass energy). The pressure in the spectrometer was typically $10^{-9}$ Torr. By combining a hybrid lens and slot aperture, the detection area was ca. 0.3 × 0.7 mm. Samples were held on a rectangular metal support by copper contact tape. Once the samples were introduced into the sample analysis chamber, they were manipulated using an actuator enabling the movement of the sample in the *x*, *y*, and *z* directions and monitored by a CCD camera. For RGD peptide gradient samples, spatial measurements were referenced to the two ends of the 10 mm × 3 mm gradient region. Ten equally separated spots along the 10-mm-long active gradient region were chosen, through software, for XPS study. After the subtraction of a linear background, all spectra were fitted using a 70% Gaussian/30% Lorentzian peak shape using the minimum number of peaks consistent with the best fit. XPS imaging data were acquired by selecting a position on the surface at which a Au/F transition existed as evidenced by the spectral data. In separate acquisitions, Au 4f photoelectrons were acquired at 84 eV, and F 1s photoelectrons, at 688 eV at medium magnification with an X-ray source power of 225 W and a resolution pass energy of 160 eV.

**Surface Plasmon Resonance (SPR) Imaging.** The apparatus for SPR imaging is similar to that described by Corn et al.[39] Light from a 100-W quartz−halogen bulb was focused and recollimated by a camera lens. The collimated light was passed through a polarizer and a narrow-band ($\lambda = 830$ nm) interference filter, and the resulting p-polarized radiation illuminated the sample at a specified incident angle. The reflected light was detected with a CCD camera and recorded on videotape. After digitizing the videotape, the images were analyzed by employing Igor (Wavemetrics, Inc.) software.

**Flow Cell Assembly.** The flow cell assembly for SPR imaging has been described in detail previously.[40] In brief, a poly(tetrafluoroethylene) (PTFE) cell was assembled with a Au/prism as one side and a stainless steel plate (counter electrode) as the other. The whole assembly was sealed by two O-rings (12.5-mm diameter). A miniature Ag/AgCl reference electrode (66-EE009), purchased from Cypress Systems, was inserted in the top of the cell and used as the reference electrode.

## Results and Discussion.

**Fluorocarbon and RGD Peptide Density Gradients.** Modifying PAA polymer thickness gradients generated density gradients of the fluorocarbon or bioactive (i.e., RGD-containing) peptide. The PAA polymer thickness gradients were formed by mapping static and dynamic electrochemical potential gradients onto Au electrodes.[23] This method is capable of forming gradients of varying dimensions. As an example, a dynamic gradient was formed on a 1-mm-long Au strip by sweeping the potential of the left end between −1500 and 100 mV versus Ag/AgCl five times and keeping the right end at a +300-mV potential offset. Figure 1a shows the transition region of a PFOA-derivatized PAA gradient as mapped by overlaying the Au 4f and F 1s XPS images. Figure 1b gives the spatial intensity profile of Au 4f and F 1s photoelectrons through the transition region. The intensity gradually decreases from left to right because of photoelectron attenuation, suggesting that the PAA polymer thickness increases accordingly from left to right. The F 1s intensity also increases from left to right, which suggests that the thicker the PAA polymer film, the stronger the F 1s intensity. The width of the transition region, measured from the fwhm of the Gaussian derivative of a fit of the Au 4f intensities to a sigmoidal function, yields 104 ± 1 μm. This result shows that the carboxylic acid functional groups inside the polymer are accessible to $H_2NCH_2(CF_2)_6CF_3$. If only the carboxylic acid groups on the surface area were accessible for modification, then the F 1s intensity would not change with polymer thickness, contrary to what is observed. It is not likely that all of the PAA carboxylic acid functional groups are modified. Crooks et al. found the coupling yield of $H_2NCH_2(CF_2)_6CF_3$ to hyperbranched PAA films to be ca. 50% based on the disappearance of the acid C=O stretching band in the reflection infrared spectrum.[36] However, the XPS imaging result demon-

(38) Lee, K. B.; Kim, D. J.; Lee, Z. W.; Woo, S. I.; Choi, I. S. *Langmuir* **2004**, *20*, 2531−2535.

(39) Nelson, B. P.; Frutos, A. G.; Brockman, J. M.; Corn, R. M. *Anal. Chem.* **1999**, *71*, 3928−3934.

(40) Zhang, Y.; Terrill, R. H.; Bohn, P. W. *Anal. Chem.* **1999**, *71*, 119−125.

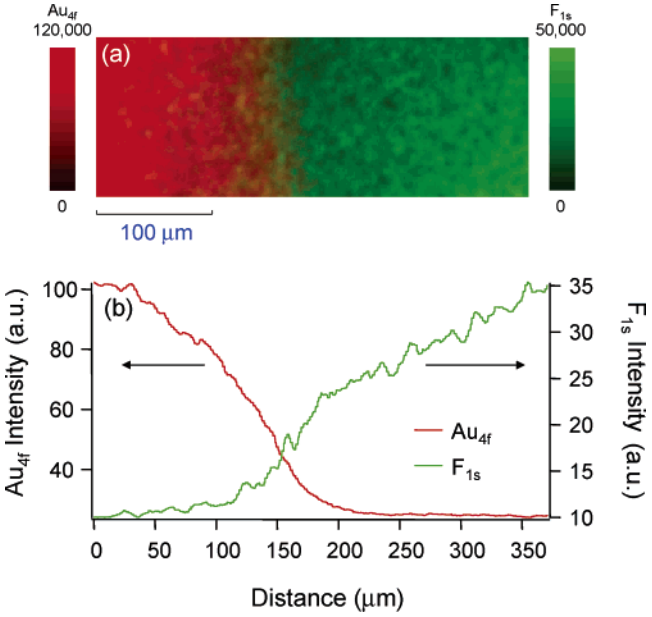


**Figure 1.** (a) XPS image showing the transition region of a PFOA-derivatized PAA thickness gradient as measured through Au 4f and F 1s XPS images. Color scales for Au (left) and F (right) are given to the side of the image. Intermediate colors represent areas of the sample with mixed Au and F signals. (b) Line scans showing the spatial distribution of the Au 4f and F 1s photoelectron intensities over the transition region.

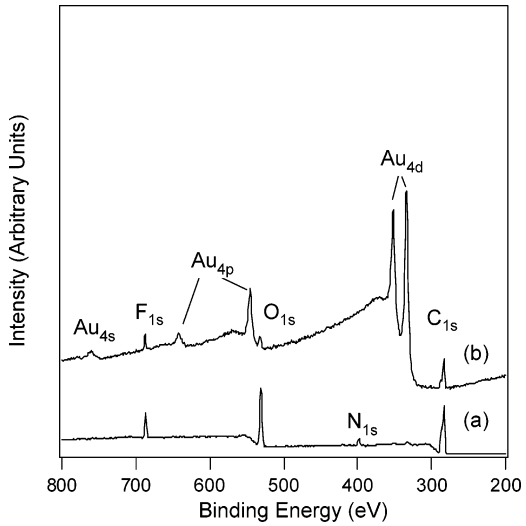


**Figure 2.** Survey scan XPS spectra of (a) an EDC/PFP-activated PAA polymer film formed by cycling (50 cycles) the applied potential of the entire electrode between −1500 and +100 mV vs Ag/AgCl and (b) an EDC/PFP-activated MUA film.

strates that it is feasible to convert PAA thickness gradients into $H_2NCH_2(CF_2)_6CF_3$ density gradients readily.

To demonstrate that a similar strategy can be used to form a density gradient of a bioactive species, a PAA gradient was formed and modified with an RGD-containing peptide (Gly-Arg-Gly-Asp-Ser-Pro-Lys). XPS was used to characterize the as-formed peptide density gradient. To achieve covalent attachment of RGD-containing peptides onto PAA polymer films, the PAA films are first activated to a common reactive intermediate, pentafluorophenol (PFP) ester, using EDC and PFP.[38] Figure 2a shows a survey scan of an activated PAA polymer film formed by cycling (50 cycles) the applied potential of the entire electrode between −1500 and +100 mV versus Ag/AgCl. The presence of the F 1s peak confirms the formation

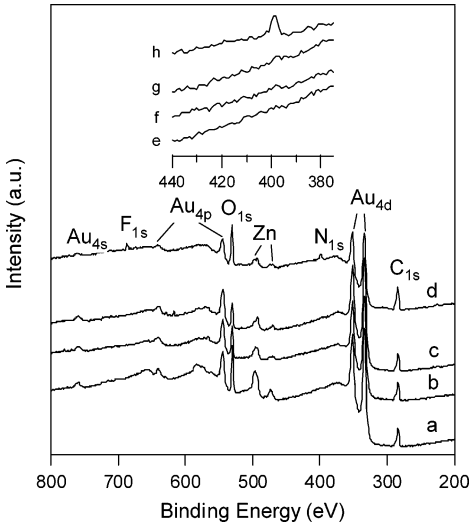


**Figure 3.** Survey scan XPS spectra of (a) PAA polymer film formed by using ethylene glycol dimethacrylate as a cross linker, (b) PEG-SH-refilled PAA polymer film, (c) RGD-peptide-soaked PAA polymer film after PEG-SH refilling but without EDC/PFP activation, and (d) RGD-peptide-soaked PAA polymer film after PEG-SH refilling with EDC/PFP activation. (e−h) Magnified XPS spectra of the N 1s region of a−d, respectively.

of the reactive pentafluorophenol ester. To estimate the conversion rate of free carboxylic acid to the reactive intermediate, a self-assembled 11-mercaptoundecanoic acid (MUA) monolayer formed on Au was activated under the same conditions. An XPS survey scan, Figure 2b, indicates Au, F, O, and C peaks in the treated MUA sample. Subsequently, high-resolution narrow region scans were performed to determine the binding energies and the relative atomic concentrations of Au, F, O, and C. The ratio of F to O is 0.624, corresponding to a ca. 25% conversion rate, given that the stoichiometric ratio of F to O is 2.50 for complete conversion. The low conversion ratio might be attributable to several factors: (1) the high density of carboxylic acid on the MUA surface combined with the steric bulk of PFP; (2) the relative lability of the intermediate PFP esters—some of them might hydrolyze before the measurement; and (3) the fact that the F 1s signal underestimates the F concentration because the C−F bond is susceptible to X-ray damage. In addition, the O 1s peak likely overestimates the intrinsic O signal due to contributions from adsorbed water.

It should be noted that the N 1s peak in Figure 2a is attributed to the cross linker, *N*,*N*′-methylenebisacrylamide. To facilitate XPS characterization of gradient samples, ethylene glycol dimethacrylate instead of *N*,*N*′-methylenebisacrylamide was used as the cross linker in forming PAA gradients to eliminate the interference in the N 1s photoelectron signal from the cross linker. Prior to RGD peptide modification, the PAA film was backfilled with PEG-SH to avoid the physical adsorption of peptide and then derivatized by sequential PFP/EDC activation and reaction with the RGD peptide. XPS was used to monitor the amide bond formation between the PAA film and the amine-terminated RGD peptide (Figure 3). Figure 3a shows a survey scan of a PAA film formed by cycling (20 cycles) the potential of the entire electrode at 50 mV/s between −1500 and +100 mV versus Ag/AgCl. Figure 3b−d shows survey scans of an as-formed PAA film refilled with PEG-SH, a PAA film soaked in RGD peptide solution after refilling with PEG-SH but without PFP/EDC activation (used to mimic physical or electrostatic absorption of RGD peptide), and a PAA film refilled with PEG-SH

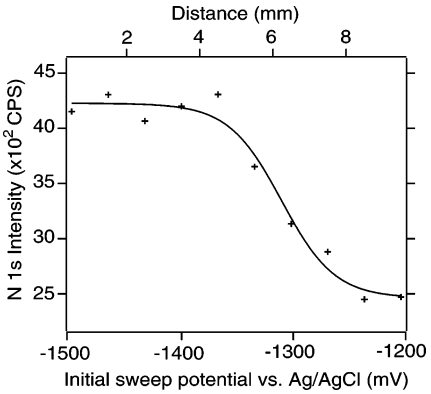


**Figure 4.** N 1s photoelectron intensity of a PAA polymer thickness gradient modified with RGD peptide. The PAA thickness gradient was formed by sweeping the potential of one end of the electrode at 50 mV/s between −1500 and 100 mV vs Ag/AgCl 20 times, while maintaining a constant +300 mV offset at the other end of the working electrode. The solid line represents a fit of the data to eq 2.

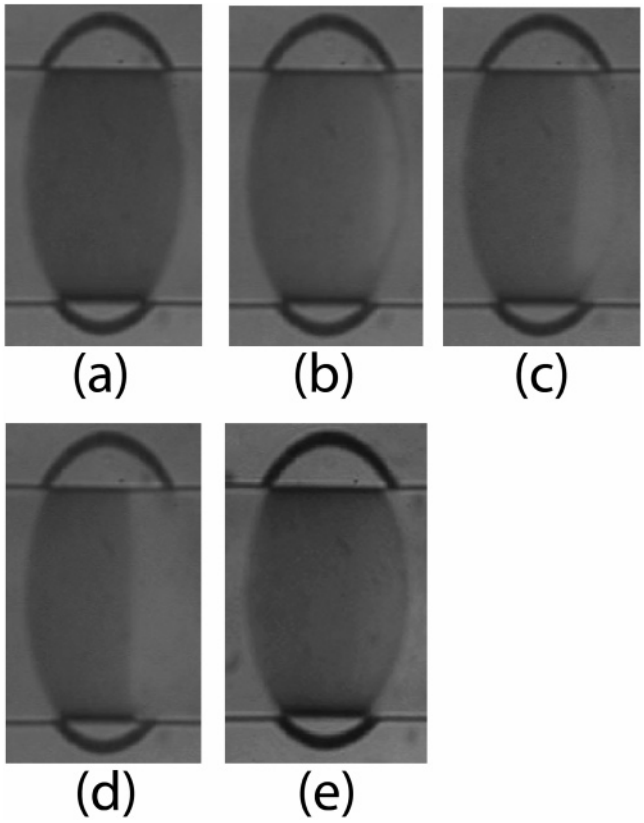


**Figure 5.** SPR images of a PAAm gradient produced by holding the left end of the working electrode at −1100 mV and the right end at −1300 mV. Images were acquired at (a) 0, (b) 6, (c) 12, and (d) 30 s. (e) SPR image after dissolving metallic Zn by exposing the PAAm film to 0.1 M HCl for 10 min.

and derivatized by sequential activation with PFP/EDC followed by reaction with the RGD peptide, respectively. The N 1s peak at ~399.5 eV in Figure 3d is attributed to N atoms in the RGD peptide, confirming the formation of RGD peptide on the surface. No detectable N 1s peak is observed in Figure 3c and g, suggesting that there is almost no physical or electrostatic absorption of RGD peptide on the surface. Finally, the presence of the F 1s peak in Figure 3d indicates that the activated PFP ester is not completely converted into an amide. However, given the steric bulk of the RGD peptide and the fact that not all of the PFP

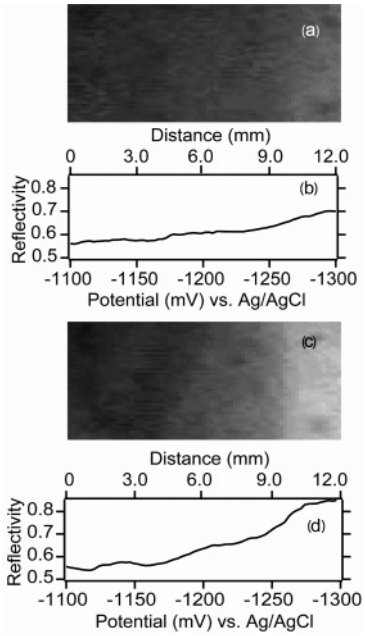


**Figure 6.** (a) SPR image of a PAAm thickness gradient acquired at 830 nm. The gradient was formed by imposing a static electrochemical potential gradient on the working electrode in which the left end was held at −1100 mV and the right end at −1300 mV for 30 s, followed by rinsing with 0.1 M HCl. (b) Line scan of the vertically averaged reflectivity of the image in part a. (c) SPR image (830 nm) of the PAAm gradient sample in part a after treatment with Au colloid solution overnight. (d) Line scan of the vertically averaged reflectivity of the image in part c.

esters would be accessible, it is not surprising that some residual PFP ester was left on the surface.

Figure 4 shows the spatial distribution of the N 1s intensity of a PAA polymer thickness gradient modified with RGD peptide. The PAA thickness gradient was formed by sweeping the potential of one end of the electrode at 50 mV/s between −1500 and 100 mV versus Ag/AgCl 20 times while maintaining a constant +300 mV offset at the other end of the working electrode. Prior to RGD peptide modification, the PAA thickness gradient was backfilled with PEG-SH to avoid the physical adsorption of peptide and then derivatized by sequential activation by PFP/EDC and reaction with the peptide, GRGDSPK. Figure 4 shows that the spatial distribution of the N 1s intensity, $I(x)$, can be fit very well with a sigmoid function of the form

$$I(x) = I_b + \frac{I_{max}}{1 + e^{(x_0 - x)/r}} \quad (2)$$

where $I_b$ is an offset, $I_{max}$ is the normalized maximum intensity, $x_0$ is the inflection point of the slope region, and $r$ is a spatial rate constant related to the slope of the gradient. Because the N 1s signal arises only from the RGD peptide, Figure 4 also represents an RGD peptide gradient on the substrate. The gradients produced here stand in contrast to the monolayer-derivatized peptide gradients produced previously in this laboratory[20,21] in that the mass of chemisorbed peptide varies with lateral position along with the thickness of the supporting PAA layer. Previously, a microfluidics photopolymerization process had been used to prepare gradient hydrogels displaying an RGD gradient for studies of cell adhesion

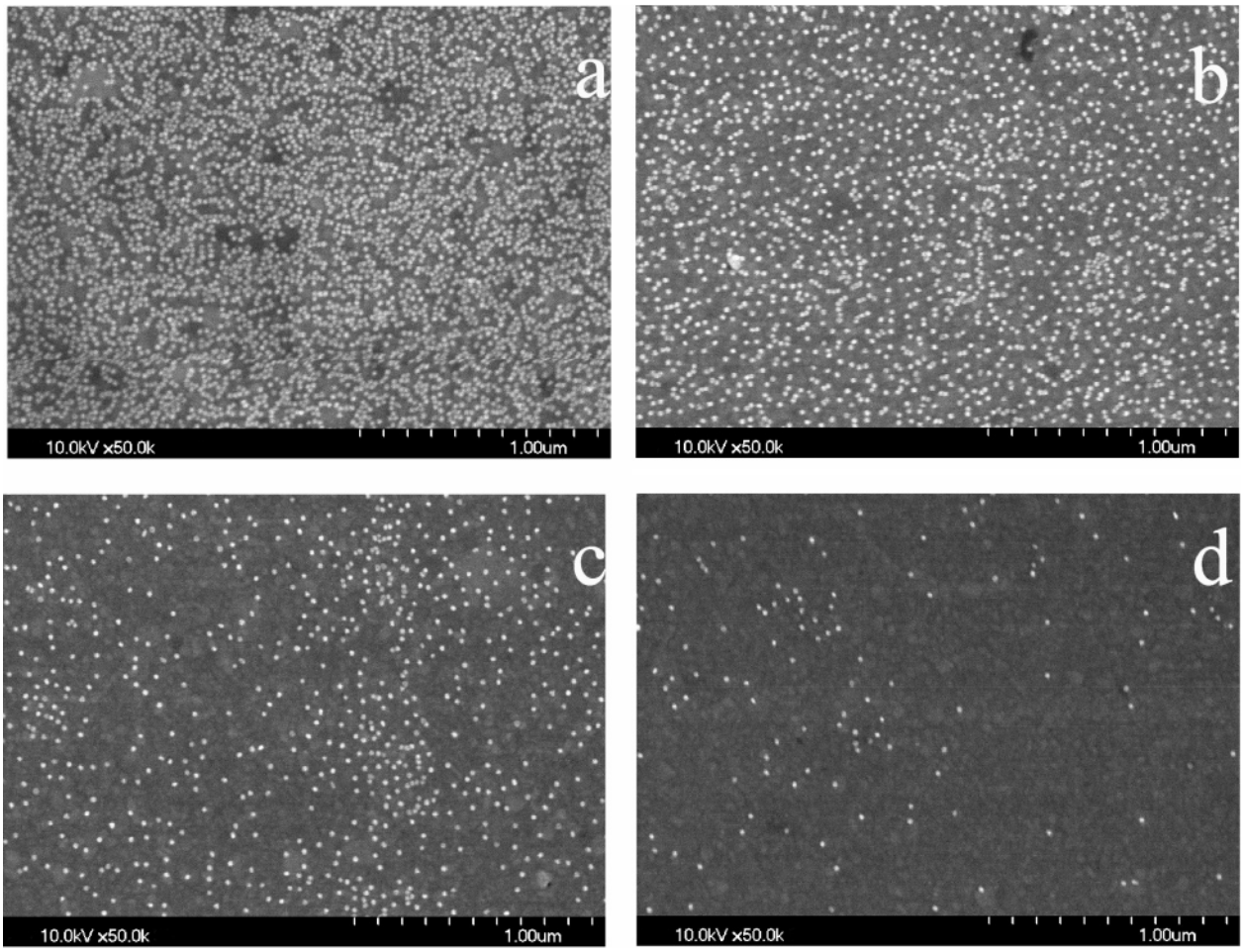


**Figure 7.** SEM images taken at positions (a) 0.5, (b) 1.0, (c) 1.5, and (d) 2.0 mm of a PAAm thickness gradient after treatment with Au colloid solution overnight. Positions are referenced to the left (large thickness) end of the PAAm gradient.

and migration.[41] The electrochemical thickness gradient formation approach described here does not require lithography and is not limited by sample size.

**PAAm Gradients Formation and Derivatization with Gold Particles.** We recently reported the preparation of PAA polymer thickness gradients through electropolymerization by mapping static and dynamic electrochemical potential gradients onto Au electrodes.[23] Here, a similar strategy was used to generate PAAm polymer thickness gradients on Au (Au-covered glass pieces and Au/prism) and ITO electrodes. The PAAm polymer was formed by electropolymerization with acrylamide as a monomer and *N*,*N*′-methylenebisacrylamide as a cross linker in a molar ratio of 50:1 in the presence of 0.1 M $ZnCl_2$ as the catalyst.

SPR imaging was used to monitor the PAAm gradient formation process in situ. Images were acquired with an incoherent white light source/narrow band interference filter combination at an incident angle corresponding to the minimum reflectance angle for bare Au. Figure 5a−d shows the temporal evolution of a PAAm gradient produced by holding the left end at −1100 mV and the right end at −1300 mV. Only the Au strip in the O-ring region was filled with solution and thus responded to the applied potential. The Figure shows that the reflectance on the right side of the Au strip, corresponding to the more negative potentials, gradually increases, whereas the reflectance on the left side exhibits little change. The transition region reaches equilibrium after 30 s, and the contrast is very clear. Because the images are acquired at the angle of the SPR resonance for bare Au, $\theta_{min,Au}$, lighter regions correspond to spatial locations where the resonance position has shifted from its bare Au position. It is reasonable to infer that the shift results from the formation of PAAm impregnated with metallic Zn. Indeed, after dissolving the Zn by exposing the film to 0.1 M HCl for 10 min, the contrast is diminished, as seen in Figure 5e.

Part a of Figure 6 shows the full SPR spatial image of a PAAm thickness gradient formed as described above, and part b is a line scan of the vertically averaged reflectivity of the image in part a. Parts a and b of Figure 6 show very little reflectance change at positions corresponding to potentials more positive than $V(x) > -1250$ mV, but the reflectance increases gradually at positions corresponding to more negative potentials (i.e., $V(x) < -1250$ mV). Bhat et al. reported that Au particles could be immobilized into PAAm brush gradients to form gold particle density gradients by simply immersing the sample in Au colloid solution.[12] Here, 20-nm colloidal Au particles ($3.5 \times 10^{11}$ particles/mL) were immobilized into the PAAm polymer gradient film by immersing it in Au colloid solution overnight. The gold particles are likely immobilized on the polymer film through physical entanglement and/or hydrogen bonding interactions between the polymer chains and the citrate surface of the nanoparticles,

(41) Burdick, J. A.; Khademhosseini, A.; Langer, R. *Langmuir* **2004**, *20*, 5153−5156.

as reported by Willner and co-workers.[42] Figure 6c shows the SPR image of the same PAAm gradient sample after treatment with Au colloid solution overnight. This image is acquired at the angle of the SPR resonance for the left end. Figure 6d is the line scan of the vertically averaged reflectivity of the image in Figure 6c. Parts c and d of Figure 6 show little reflectance change at positions corresponding to potentials more positive than −1160 mV, and then the reflectance increases at positions corresponding to more negative potentials in the range of −1160 mV > $V(x)$ > −1250 mV, exhibiting the largest reflectance increases at potentials negative of −1275 mV. Compared to parts a and b of Figure 6, the contrast of the SPR image after Au nanoparticle immobilization is much higher, as expected. The enhanced contrast of the SPR resonance resulting from Au particle immobilization suggests that the loading of Au particles per unit area is higher in thicker regions of the PAAm film than in thinner PAAm film regions. Nanoparticle enhancement of SPR contrast has been reported before, and the signal amplification was explained by the interaction of localized, propagating surface plasmons.[43−45] This phenomenon is especially well suited to characterizing 3D gradients of composite materials because the contrast scales with the volume occupied by the evanescent electric field on the dielectric (PAAm−Au) side of the interface.

To better understand the morphology of PAAm thickness gradients derivatized with Au colloids, scanning electron microscopy (SEM) was used to probe Au nanoparticle-decorated PAAm thickness gradients. The PAAm sample was formed by imposing a dynamic potential gradient on a 3-mm-long thin Au stripe in which the left end sweeps between −1500 mV < $V(x)$ < +100 mV five times while maintaining a +200 mV potential offset on the right end, followed by rinsing with 0.1 M HCl and then soaking in 20-nm Au colloid ($3.5 \times 10^{11}$ particles/mL) solution overnight. Panels a−d of Figure 7 show SEM images of a PAAm gradient with attached Au particles 0.5, 1.0, 1.5, and 2.0 mm from the large thickness end of the PAAm gradient, respectively. On the basis of these SEM images, the area density of Au particles is measured to be 1350, 500, 120, and 40 particles/$\mu$m$^2$ at positions of 0.5, 1.0, 1.5, and 2.0 mm, indicating that the density of gold particles is higher in the thicker regions of the PAAm film formed at more negative potentials. This result is consistent with the SPR imaging result of a PAAm gradient film treated with gold particles.

A key question regarding these Au−PAAm materials concerns whether the Au nanoparticles are confined to the surface or are distributed throughout the volume of the PAAm film. To investigate this question, Au−nanoparticle/PAAm density gradients were formed on a transparent conductive substrate, ITO-coated glass, for UV−visible absorbance measurements. The hypothesis is that if the Au particles are surface-confined then the magnitude of the Au nanoparticle absorbance should be independent of PAAm thickness (i.e., it should be spatially invariant across a PAAm thickness gradient). Figure 8 shows an example of a set of spatially resolved UV−visible absorbance spectra of a PAAm thickness gradient film, formed by the dynamic gradient approach, on ITO after soaking in 16-nm-diameter Au colloid overnight. The top spectrum was collected on the thick PAAm side of the gradient, and the sample was shifted 3 mm for each subsequent spectral measurement. Each absorption spectrum can be deconvoluted into three peaks: one around 530 nm, which is close to the plasmon absorbance ($\lambda \approx 520$ nm) of individual particles, and two more near 600 and 630 nm at low Au particle loading but shifting by ~20 nm to near 620 and 650 nm at the highest loadings. These red-shifted peaks are caused by interparticle coupling, which results from increased particle density.[46] In addition to this spectral shift, the magnitude of both the individual particle plasmon absorbance and the interparticle coupled-plasmon absorbance increases by ca. 50% on going from the low thickness to high thickness end of the Au−PAAm gradient. Furthermore, the scattering background for the two positions on the thickest end of the PAAm gradient are much larger, as would be expected if the Au nanoparticles are distributed throughout the volume of the film. On the basis of these results, it is likely that the Au particles are distributed throughout the volume of the polymer film instead of being attached only to the surface.

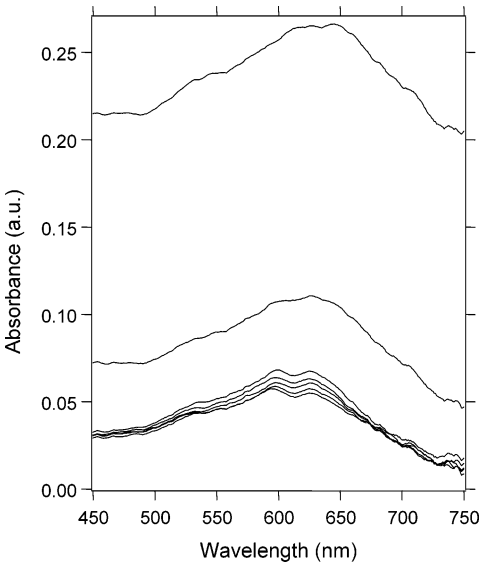


**Figure 8.** Spatially resolved UV−visible absorbance spectra acquired from a 2.5-cm-long thickness gradient of PAAm film on an ITO substrate after soaking in 16-nm-diameter Au colloid overnight. This gradient was formed by applying a dynamic potential gradient to the 2.5-cm-long ITO substrate in which one end was swept between −1500 and 100 mV five times, while maintaining a +300 mV potential offset on the right end, and then soaking in 16-nm Au colloid ($3.5 \times 10^{11}$ particles/mL) overnight. The top spectrum was collected on the high-density side of the gradient (the thickest polymer side), and the sample was shifted 3 mm for each consecutive spectral measurement. The offsets for the topmost two spectra represent the observed scattering background and are real features of the data.

## Conclusions

Anisotropic thickness gradient hydrogel films offer a unique route to the preparation of laterally graded 3D composite materials. This capacity was explored here by coupling both static- and dynamic-potential gradient films of PAA and PAAm to chemically useful derivatizing agents. Density gradients of amino-terminated molecules can be prepared by derivatizing laterally varying thickness gradients of PAA by the formation of amide linkage. This procedure provides a general route to the insertion of various functionalities, but particular interest accrues for

(42) Pardo-Yissar, V.; Gabai, R.; Shipway, A. N.; Bourenko, T.; Willner, I. *Adv. Mater.* **2001**, *13*, 1320−1323.
(43) Hutter, E.; Fendler, J. H.; Roy, D. *J. Phys. Chem. B* **2001**, *105*, 11159−11168.
(44) Lyon, L. A.; Pena, D. J.; Natan, M. J. *J. Phys. Chem. B* **1999**, *103*, 5826−5831.
(45) Lyon, L. A.; Musick, M. D.; Natan, M. J. *Anal. Chem.* **1998**, *70*, 5177−5183.
(46) Grabar, K. C.; Freeman, R. G.; Hommer, M. B.; Natan, M. J. *Anal. Chem.* **1995**, *67*, 735−743.

the use of biological molecules, as exemplified by the GRGDSPK peptide used in these studies. By exploiting the same basic synthetic steps, density gradients of fluorocarbons were formed to demonstrate the capacity to alter the surface tension ex post facto. Gold nanoparticles were also used to modify thickness gradients of PAAm. On the basis of SPR, SEM, and UV−visible absorption results, the Au particles are distributed throughout the volume of the PAAm film, illustrating that true 3D composite materials can be prepared even when the derivatizing agent is supermolecular in size.

**Acknowledgment.** This work was supported by the National Science Foundation through grant CHE 0451661. The Center for Microanalysis of Materials is partially supported by the Department of Energy through grant DE FG02 91ER45439.

**Supporting Information Available:** An SPR imaging movie of poly(acrylamide) gradient formation on a Au/prism structure. This material is available free of charge via the Internet at http://pubs.acs.org.

LA0580053